Summary: Experiment

Jana Bielčíková[1,2,*]

[1]Nuclear Physics Institute, Czech Academy of Sciences, 250 68, Řež, Czech Republic
[2]FNSPE, Czech Technical University in Prague, Břehová 7, 115 19, Czech Republic

Abstract. This proceedings summarizes the experimental results presented at the QM2025 conference along with an outlook on future experimental programs.

The Quark Matter conference series has a rich and somewhat organic history, shaped by entwined developments in theory and experiment that converged in the early 1980s. As H. Satz and R. Stock recalled in their proceedings of the 25th QM conference [1], the 1982 meeting in Bielefeld, following a 1980 theory symposium in Bielefeld and an experimental workshop at the GSI Darmstadt, marked the first dedicated forum for exploring the thermodynamics of strong interaction matter through high-energy nuclear collisions. Since then, the conference has grown not only in size, but also in the scope and complexity of the physics observables studied, transforming the investigation of the QGP from its "nebulous beginning" [1] in the 1980s, into a field of precision science. This year's conference, held in Frankfurt, brought the series back to Germany, not far from the locations where its earliest steps were taken.

1 Search for QCD critical point

A central goal of heavy-ion physics has long been the search for a possible QCD critical point (CP) associated with the 1st order phase transition. At the conference, STAR presented high-precision measurements of net-proton factorial cumulants and their ratios from the RHIC BES-II program ($\sqrt{s_{NN}}$ = 7.7–27 GeV), corresponding to baryochemical potential μ_B = 400–150 MeV [2]. Compared with non-critical baseline calculations, a minimum in the net-proton cumulant ratio C_4/C_2 (Fig. 1) is observed, deviating by about 2–5σ around $\sqrt{s_{NN}}$ = 19.6 GeV. Although this resembles the expected CP behavior, dynamical models including critical effects are needed to interpret the data. STAR also reported fixed-target results ($\sqrt{s_{NN}}$ = 3.0–7.7 GeV), extending the search to higher baryochemical potential, where C_4/C_2 remains consistent with UrQMD predictions without critical effects included. Before RHIC concludes operations, it is essential that STAR acquire additional fixed-target data near $\sqrt{s_{NN}}$ = 4 GeV to clarify the energy dependence relevant to the CP search. Ongoing searches at NA61/SHINE [3, 4] and HADES [5, 6] likewise remain inconclusive.

2 Spin related phenomena

The velocity and vorticity fields in the evolving QGP are expected to polarize produced particles via spin–orbit coupling. In non-central collisions, the initial shear generates a net "global

*e-mail: bielcikova@ujf.cas.cz

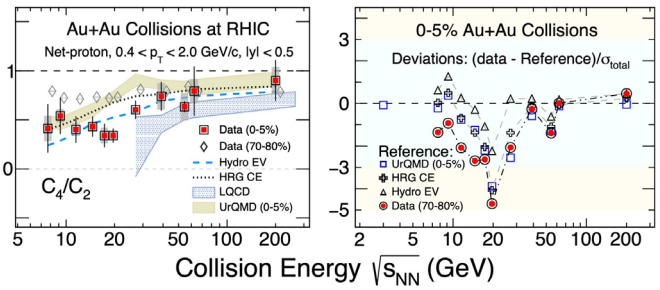

Figure 1. Net-proton cumulant ratio C_4/C_2 together with the significance of deviation (data−reference)/σ_{total} measured by STAR during the RHIC BES-II program. Figure adopted from [2].

polarization" of particles along the system's orbital angular momentum. Recent Λ-hyperon polarization measurements have opened new avenues to study QGP spin dynamics. New BES-II STAR results with greatly reduced uncertainties confirm that Λ polarization decreases with increasing beam energy, show no significant splitting between Λ and $\bar{\Lambda}$, and place an upper limit on the late-stage magnetic field of $B \leq 10^{13}$ T. Similar behavior, though with larger uncertainties, was also reported for Ξ and Ω [7]. Polarization may also occur along the beam axis, where anisotropic flow generates vorticity and induces "local" polarization. STAR BES-II measurements of Λ and $\bar{\Lambda}$ local polarization $P_{2,z}$ (Fig. 2, left), motivated by the predicted baryonic spin Hall effect, show no strong energy dependence, underscoring the need for simultaneous fits to global and local polarization. In p+Pb collisions, CMS observed a significant positive Λ polarization $P_{z,s2}$ (Fig. 2, right) [8], challenging models.

We conclude the selection of spin-related results with a novel measurement probing the transition from quark pairs to hadrons, directly addressing the problem of confinement. It exploits spin correlations of $\Lambda\bar{\Lambda}$ pairs, tracing them to their entangled $s\bar{s}$ origin where spins are expected to align. Interactions with the QCD medium during hadronization can induce decoherence of this entanglement, offering a new probe of QCD dynamics. The STAR data show the first evidence of $\Lambda\bar{\Lambda}$ spin correlation in pp collisions at $\sqrt{s} = 200$ GeV, with a relative polarization of (18±4)% linking entangled quark pairs in the vacuum to their hadronic states [9]. The correlation disappears at large angular separations, consistent with decoherence.

3 Exploring the limits and origins of collectivity

Precise measurements from the LHC and RHIC presented, now let us tackle key open questions related to collectivity: up to what transverse momentum (p_T) hadrons flow, what is the origin of collectivity in small systems, and what is physics interpretation of it.

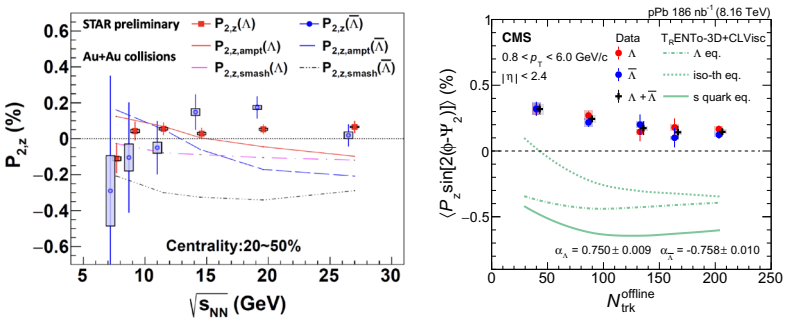

Figure 2. Dependence of local Λ polarization on energy in Au+Au collisions from STAR (left) and multiplicity in p+Pb collisions at $\sqrt{s_{NN}} = 8.16$ TeV by CMS (right). Figures adopted from [7] and [8].

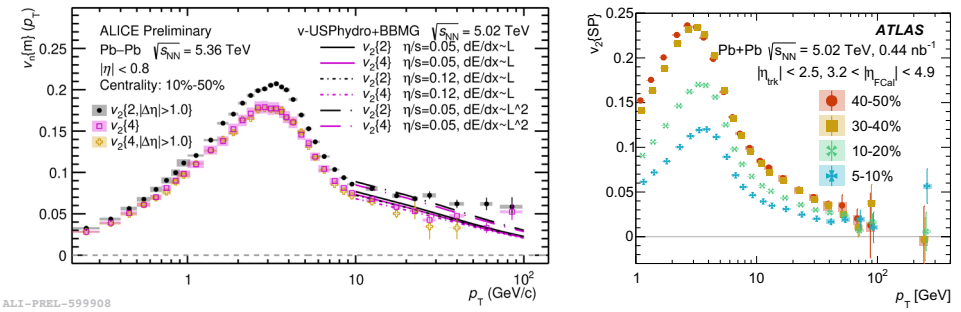

Figure 3. Transverse momentum dependence of v_2 in Pb+Pb collisions from ALICE Run 3 (left) and ATLAS (right). Figures taken from [10, 11].

Both ALICE [10] and ATLAS [11] measured elliptic (v_2) and triangular (v_3) anisotropies of charged particles produced in Pb+Pb collisions with unprecedented precision to very high p_T. The observed positive values up to $p_T \approx 100$ GeV/c for v_2 (Fig. 3) and 25 GeV/c for v_3, respectively, suggest that the parton energy loss in QGP is influenced by the event-by-event initial geometry and the data can be used to constrain the path-length dependence of jet quenching. The baryon–meson grouping observed in heavy-ion collisions from LHC energy [12] down to top RHIC energies, commonly regarded as a signature of partonic collectivity, breaks down around $\sqrt{s_{NN}} = 4.5$ GeV [13], offering new insight into how the onset of the QGP depends on collision energy, although this interpretation may not be unique.

Small collision systems have revealed unexpected features in recent years, and the conference provided new insights into the origin of long-range correlations and collectivity. ALICE reported ultra-long-range two-particle azimuthal correlations with pseudorapidity separation $|\Delta\eta| > 5$ in both pp and p+Pb collisions [14] (Fig. 4). Neither hydrodynamic calculations, CGC-based models, nor PYTHIA with string shoving reproduce the signal, placing strong constraints on theoretical descriptions of collective-like effects across multiplicities. LHCb measured v_2 in p+Pb collisions at forward/backward rapidities, observing an increase with multiplicity but no beam-direction dependence, suggesting limited initial-state effects [15]. The results, generally below hydrodynamic predictions, provide key input for understanding collectivity and longitudinal dynamics in small systems. At RHIC, O+O collisions have now been studied, offering further insight into the onset of collectivity. STAR presented v_2 and v_3 in d+Au and O+O collisions scaled by eccentricity (Fig. 5). The consistent scaling in both systems indicates a common mechanism translating initial geometry into final-state flow, de-

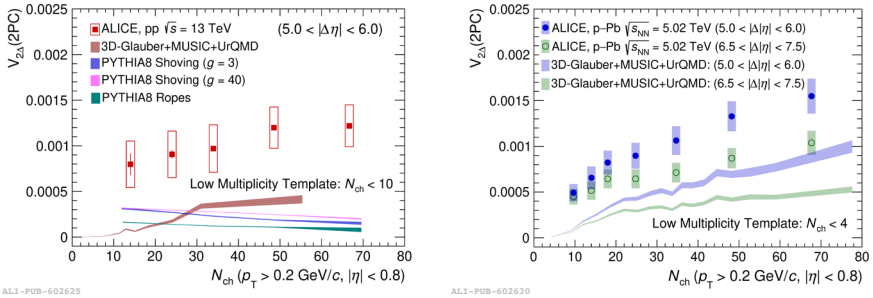

Figure 4. Multiplicity dependence of v_2 from two-particle correlations in pp and p+Pb collisions with large $|\Delta\eta|$ separation measured by ALICE at $\sqrt{s_{NN}} = 5.02$ TeV. Figures adopted from [14].

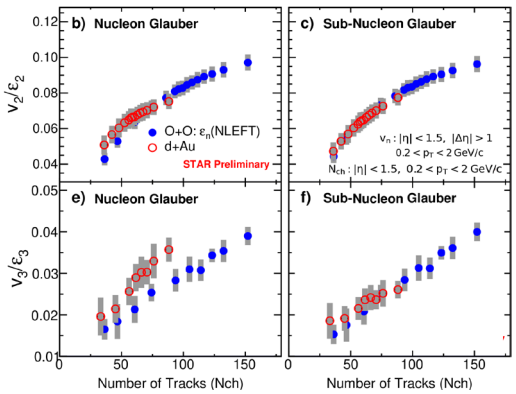

Figure 5. Multiplicity dependence of elliptic (v_2) and triangular (v_3) flow scaled with initial-state eccentricity (ϵ_n) from a nucleon-Glauber model and a sub-nucleon (quark) Glauber model in O+O and d+Au collisions at $\sqrt{s_{NN}}$ = 200 GeV measured by STAR. Figure adopted from [16].

spite similar multiplicities from different initial configurations. The data favour a sub-nucleon Glauber model [16], supporting a geometry-driven interpretation. The upcoming LHC run with O+O and Ne+Ne collisions, together with new LHCb SMOG2 capabilities for flexible targets and energy scans, will further probe these effects at higher energies. Another probe of QGP and its expansion dynamics is the radial flow, which has received attention through p_T-differential radial-flow fluctuations $v_0(p_T)$, which, unlike v_2 that is primarily sensitive to shear viscosity, probe the bulk viscosity [17]. ATLAS measured $v_0(p_T)$ for charged particles in Pb+Pb collisions, observing long-range pseudorapidity correlations, p_T factorization, and a centrality-independent shape [18]. ALICE reported results for inclusive charged particles and identified π, K, and protons [19], showing low-p_T mass ordering consistent with hydrodynamic flow and, at higher p_T, a baryon–meson splitting suggestive of quark recombination. Together, these measurements confirm the collective nature of radial flow and provide complementary constraints on QGP transport properties.

4 Hyperon-nucleon and many-body interactions

Femtoscopic correlations, originally used to study the size and lifetime of the particle-emitting source, now provide new insights into the fundamental interactions between hyperons and nucleons as well as many-body interactions, important for understanding the structure of hypernuclei, searching for exotic multiquark states or understanding neutron star EoS. Using measurements of d–Λ correlations in Au+Au collisions at $\sqrt{s_{NN}}$ = 3 GeV, STAR reported new results on the binding energy of ${}^{3}_{\Lambda}$H. The measured value, $0.06^{+0.06}_{-0.02}$ MeV/c^2, corresponds to a radius of approximately 16 ± 5 fm, consistent with the world average but with notably smaller uncertainty [21]. The study of exotic multi-quark states, especially strange dibaryons, is challenging due to short lifetimes and difficulty distinguishing them from scattering states.

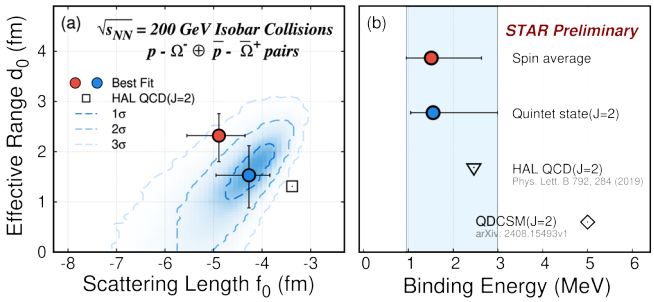

Figure 6. $p - \Omega^-$ scattering length (f_0) and effective range (d_0) from spin-averaged and quintet methods (left) and the respective binding energy (right) of dibaryon state measured by STAR in isobar collisions at $\sqrt{s_{NN}}$ = 200 GeV. For details see [20].

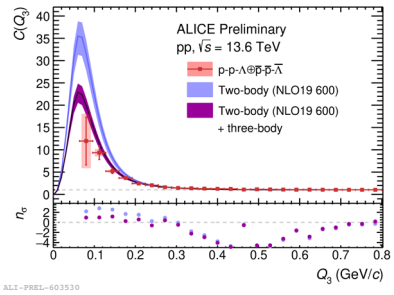

Figure 7. p-p-Λ femtoscopic correlations measured by ALICE in pp collisions at $\sqrt{s}$ = 13.6 TeV compared calculations. For details see [22].

STAR presented measurements of the $p-\Xi^-$ and $p-\Omega$ correlations, where the latter shown in Fig. 6 are featuring a shallow bound state, with a binding energy $E = 1.6^{+1.4}_{-0.5}$ MeV (3.2σ, spin $J = 2$), indicating formation and possibly the first evidence of a strange dibaryon [20].

Λ–nucleon interactions are essential for modeling neutron-star cores, where strangeness may appear, yet short-range two- and three-body forces remain poorly constrained even at saturation density. Femtoscopic correlations in high-energy pp collisions could provide a unique probe of three-hadron dynamics beyond conventional scattering experiments. ALICE demonstrated the feasibility of such studies (Fig. 7) [22], and upcoming high-statistics data are expected to constrain models, with initial predictions already available for p–p–p and p–p–Λ systems.

5 Electromagnetic probes: Photons and dileptons

Photons and dileptons serve as unique probes, escaping the medium without strong interactions and carrying information from all collision stages, from early hard scatterings to thermal radiation of the QGP and hadronic phase. Dilepton spectra reveal in-medium vector meson modifications, while both probes constrain the system's temperature and space–time evolution. For some time, calculations struggle to explain simultaneously direct γ spectra and v_2, which culminated in the so called 'direct photon puzzle': observed large yield points to early emission time at higher T, large v_2 in contrast to late emission and lower T. PHENIX pre-

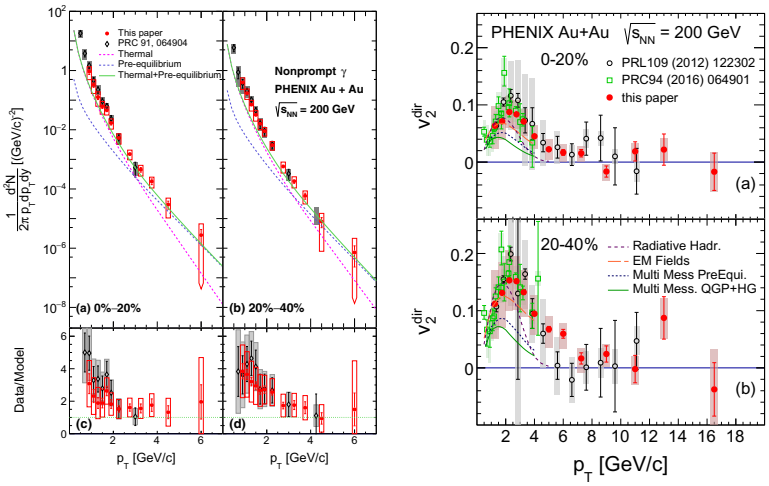

Figure 8. Multiplicity dependence of integrated direct-photon yield (1–5 GeV/c) (left) and v_2 (right) in Au+Au collisions at $\sqrt{s_{NN}}$ = 200 GeV measured by PHENIX. Figures adopted from [23, 24].

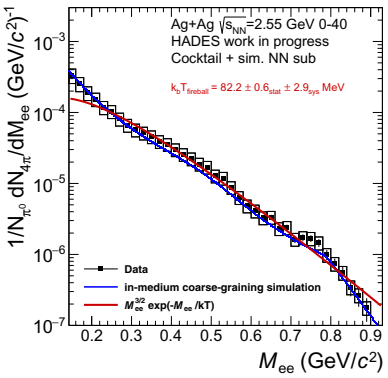

Figure 9. Invariant mass of dielectron thermal excess pairs in Ag+Ag collisions at $\sqrt{s_{NN}}$ = 2.55 GeV measured by HADES [5].

sented measurement of direct-γ v_2 in Au+Au collisions at $\sqrt{s_{NN}}$ = 200 GeV [24] shown in Fig. 8 with improved statistics and higher p_T reach. Above $p_T \approx$ 8–10 GeV/c, where hard scattering dominates direct-γ production, v_2 is consistent with zero, while at lower p_T it follows that of π^0s, though somewhat smaller. Although calculations have improved over time, no model fully explains the data. The conference once again emphasised a tension between a tension between PHENIX [23] and STAR [25] integrated non-prompt direct γ yields, which follow a power-law dependence on multiplicity but scale differently when combined with ALICE data [26], requiring resolution.

We now turn to dilepton measurements and the extracted temperature, a fundamental yet still poorly constrained quantity. Following major upgrades, HADES presented dilepton spectra and related thermal dilepton excess in Ag+Ag collisions at $\sqrt{s_{NN}}$ = 2.42 and 2.55 GeV [5] (see Fig. 9), further extending measurements in Au+Au collisions [27]. The measured average fireball temperatures are well above universal freeze-out region. STAR reported new dilepton results from the BES-II [28] and isobar data, finding, in the low-mass region (ρ^0 dominated), temperatures consistent with statistical hadronization [29] and the critical T_c from lattice QCD [30, 31], while in the QGP dominated intermediate-mass region $T \sim$ 300 MeV. ALICE has reported the first dielectron spectrum in pp collisions at $\sqrt{s}$ = 13.6 TeV [32]. The improved resolution allows prompt and non-prompt sources to be separated using DCA template fits, an important step toward isolating QGP thermal radiation in future LHC runs. A similar DCA-based method has been demonstrated at RHIC by PHENIX[33].

6 Unraveling different QCD scales with jets

Jet quenching has been studied for more than two decades, evolving from early observations of high-p_T hadron suppression to detailed investigations of fully reconstructed jets and their substructure. These efforts aim to disentangle the underlying mechanisms of quenching and to clarify the roles of medium recoil and medium response across different collision energies and systems. At the conference, many new results were presented. Notably, LHCb reported the first direct observation of the dead-cone effect in beauty-quark jets [34], following ALICE's earlier measurement in charm-initiated jets [35]. These results, based on detailed analyses of the Lund jet plane in pp collisions at $\sqrt{s}$ = 13 TeV, provide a precision test of QCD. New ALICE results also highlighted the strong potential of Run 3 data, showing significant improvements over Run 2, particularly those involving charm-tagged jets. Last but not least, STAR presented first measurements of jet quenching signal in O+O collisions at $\sqrt{s_{NN}}$ = 200 GeV [36]. If confirmed, this would represent the first observation of jet quenching in a small collision system.

Recently, energy–energy correlators (EECs) have been proposed as complementary probes of both perturbative and non-perturbative QCD, offering sensitivity to color coher-

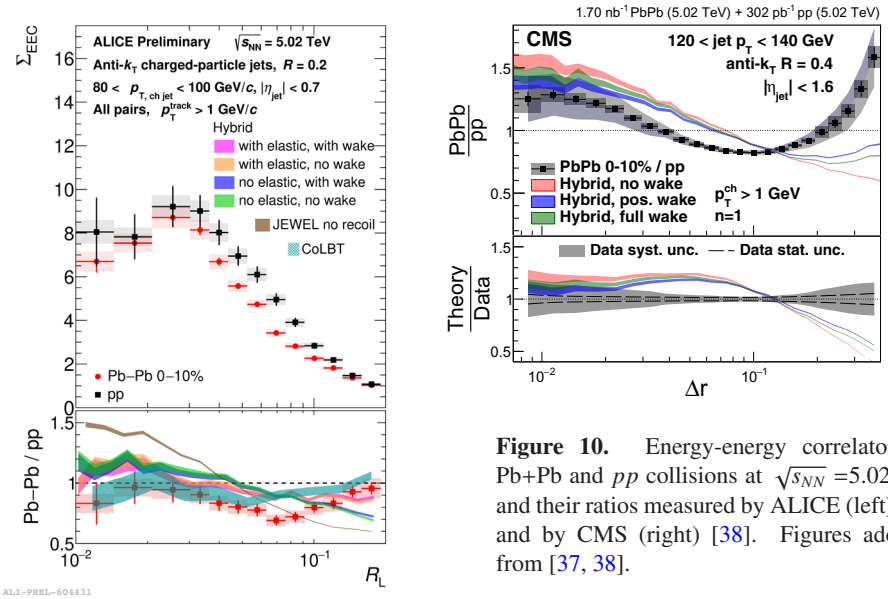

Figure 10. Energy-energy correlators in Pb+Pb and pp collisions at $\sqrt{s_{NN}}$ =5.02 TeV and their ratios measured by ALICE (left) [37] and by CMS (right) [38]. Figures adopted from [37, 38].

ence, where gluons radiate independently above a critical angle, and to the "jet wake," in which a high-p_T parton drags medium particles. ALICE and CMS reported significant modification of EECs in central Pb+Pb relative to pp collisions displayed in Fig. 10. Models including color coherence or medium response predict qualitatively similar modifications. A new prediction from the Hybrid Model [41] discussed at the conference strongly motivates ALICE to extend their measurement by lowering the track-p_T threshold to 150 MeV/c and studying separations larger than the jet radius R, which cannot come from two hard core partons, to look for enhancement that would signal the jet wake. ATLAS has also studied jet substructure using the Soft Drop angle dR_{12} in $R = 1$ jets from $R = 0.2$ subjets. The nuclear modification factor R_{AA} (Fig. 11) decreases with dR_{12} and plateaus for $dR_{12} \geq 0.2$. Comparison with the Hybrid Model [39] favors a finite medium resolution length, $L_{\rm res} \sim (1\text{–}2)/(\pi T)$, providing the first quantitative bounds.

Unlike strongly interacting particles, photons and Z bosons traverse the QGP without significant modification, making them clean probes of the initial hard scattering and providing a determination of the hard-scattering scale. We highlight here the CMS correlations of charged-hadrons with Z boson in Pb+Pb collisions for three different p_T ranges of charged-

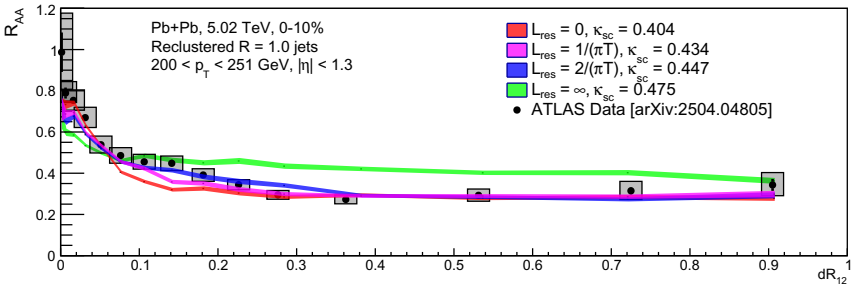

Figure 11. $R_{\rm AA}$ as a function of dR_{12} for $R = 1$ jets constructed from skinny reclustered subjets reclustered and the Soft Drop grooming procedure compared with Hybrid Model. Figure adopted from [39].

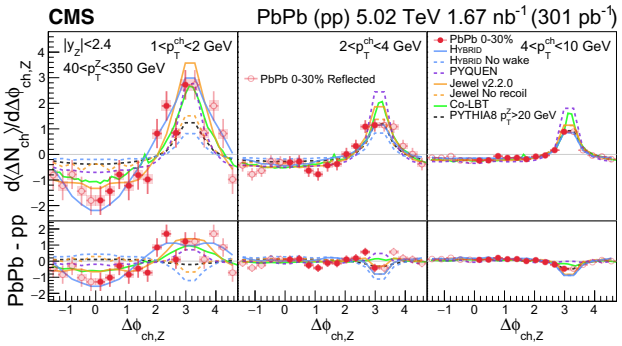

Figure 12. Z-hadron azimuthal correlations as a function of hadron p_T in Pb+Pb collisions at $\sqrt{s_{NN}}$ = 5.02 TeV measured by CMS together with the respective differences relative to pp collisions and model calculations. Figure adopted from [40].

hadron momenta shown in Fig. 12. For charged hadrons with p_T= 1–2 GeV/c, the distributions manifest a dip at small angular separation $\Delta\phi_{\mathrm{ch,Z}} \sim 0$ accompanied by an excess at $\Delta\phi_{\mathrm{ch,Z}} \sim \pi$ with significance of 3σ. This observation is consistent with expectations of a hydrodynamic wake created as the QGP is depleted of energy by the hard parton propagating through it. Models that omit medium–response effects fail to describe the data, whereas those that incorporate medium response achieve significantly better agreement. However, the current statistical uncertainties do not yet permit more definitive conclusions.

We conclude the section with studies of jet hadrochemistry. As discovered at RHIC and confirmed at the LHC, baryon-to-meson ratios are strongly enhanced at intermediate p_T = 2–5 GeV/c in heavy-ion compared to pp collisions, commonly attributed to strong hydrodynamic flow and parton recombination in the QGP, though it remains to be seen whether a similar effect occurs in jets. ALICE [42] and STAR [43] measurements of proton-to-pion (p/π) and pion-to-kaon (π/K) ratios, show no significant p/π enhancement in Au+Au collisions at RHIC, but the LHC data suggest possible baryon and strangeness enhancement at intermediate p_T in Pb+Pb collisions. More precise determinations will require higher statistics and additional identified particle species to constrain jet hadrochemistry modifications.

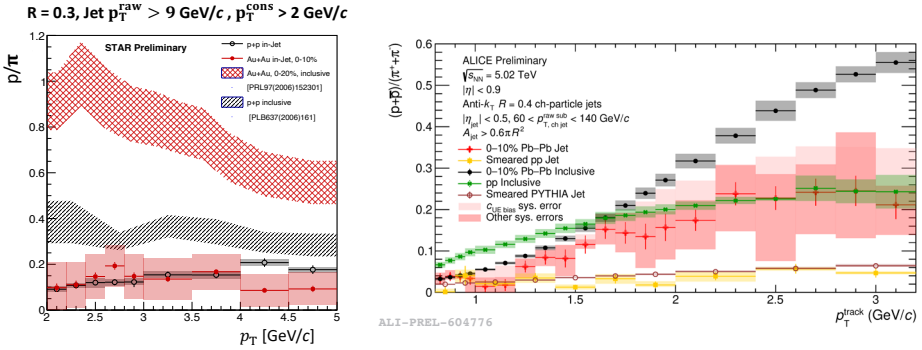

Figure 13. In-jet p/π ratios in Au+Au ($\sqrt{s_{NN}}$ = 200 GeV) by STAR [43] (left) and Pb+Pb collisions ($\sqrt{s_{NN}}$ = 5.02 TeV) by ALICE [42] compared with the pp data. Figures adopted form [42, 43].

7 Quarkonia and open charm production

Also in the open heavy-flavor and quarkonium sector, many new measurements were presented. Starting with open charm, ALICE has performed the first reconstruction of B^0 mesons

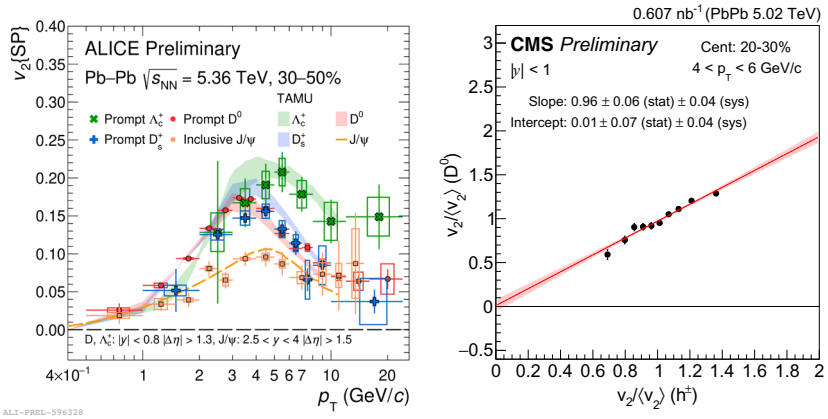

Figure 14. (Left) v_2 of D^0, D^+, D_s^+, J/ψ, and Λ_c^+ in Pb+Pb collisions at $\sqrt{s_{NN}}$ = 5.36 TeV measured by ALICE [44]. (Right) Correlation between the normalized v_2 of D^0 and hadrons in semi-central Pb+Pb collisions at $\sqrt{s_{NN}}$ = 5.02 TeV by CMS [45]. Figures adopted from [44, 45].

in Run 3, thanks to its improved inner tracker resolution, completing the mapping of the beauty production cross section at LHC energies down to low p_T. At the lower SPS energies, NA61/SHINE reported the first-ever measurement of open charm production at SPS energy, in Xe+La at $\sqrt{s_{\rm NN}}$ = 16.8 GeV, enabled by upgraded vertexing capabilities using the detector prototype [3]. The data pose a clear challenge to models as microscopic approaches tend to underestimate the yields, while statistical hadronization models overestimate them. Upcoming high-statistics Pb+Pb data are expected to provide further insight into charm production in this energy regime.

Recent heavy-ion data also reveal clear collectivity in charm production, indicating strong coupling of c quarks to the medium. ALICE presented new v_2 data of charm-hadrons down to low p_T along with the first v_2 measurement for a charmed baryon Λ_c (Fig. 14) [44]. As for light-flavor hadrons, a mass hierarchy and baryon-meson splitting at intermediate p_T is present. Separating prompt and non-prompt contributions to D^0 and Λ_c v_2, reveals a stronger degree of equilibration for c than for b quarks. To study the role of initial-state geometry, CMS measured the v_2 of prompt D^0 mesons in Pb+Pb collisions using event-shape engineering [45]. The linear correlation between the v_2 of prompt D^0 mesons and of low-p_T charged particles across centrality (Fig. 14), indicates that the c-quark flow is primarily driven by the initial-state geometry. At high p_T, existence of small deviations could hint at additional mechanisms such as path–length dependent energy loss. Overall, these observations reinforce the picture that also c and b quarks experience significant rescattering and partial thermalization in the QGP, offering a powerful probe of the transport properties of the medium.

Quarkonia measurements continue to provide precise probes of medium effects, refining our understanding of suppression and regeneration mechanisms. We highlight some of the new measurements of excited quarkonia states, motivated by suppression patterns not fully explained by initial-state effects and serving as sensitive probes of possible final-state effects, including the formation of a QGP droplet in small collision systems. For the first time in p+A collisions, CMS observed a statistically significant multiplicity-dependent suppression of prompt $\psi(2S)$ relative to J/ψ production in p+Pb collisions at $\sqrt{s_{\rm NN}}$ = 8.16 TeV [46], while non-prompt production shows no trend (Fig. 15 left). These results indicate final-state effects preferentially dissociating weakly bound states, consistent with co-mover interactions or possible QGP formation and providing valuable input for models. At forward rapidity, the prompt $\psi(2S)$ to J/ψ ratio in p+Pb collisions (Fig. 15 right) [47] matches pp results,

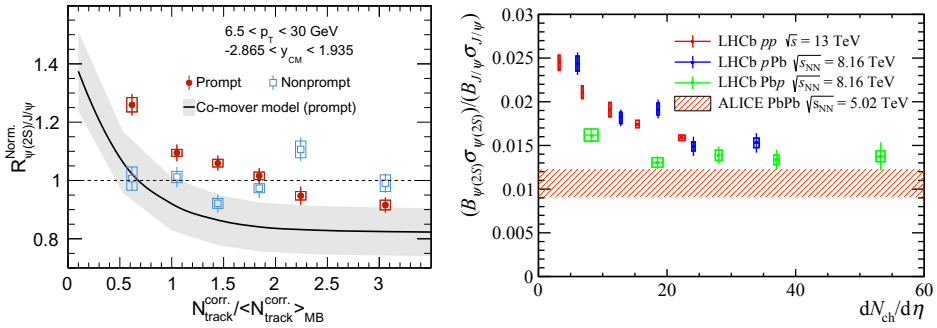

Figure 15. (Left) Multiplicity dependence of the prompt and non-prompt $\psi(2S)$-to-J/ψ cross section ratio measured by CMS in p+Pb collisions at $\sqrt{s_{NN}}$ = 8.16 TeV. (Right) Comparisons of the same ratio in pp, p+Pb, Pb+p from LHCb with Pb+Pb collisions from ALICE [50]. Figures adopted from [46, 47].

while Pb+p shows a trend closer to Pb+Pb data, suggesting additional mechanisms beyond co-mover effects. Looking ahead to Run 3, the new muon forward tracker (MFT) extends ALICE capabilities to separate prompt and non-prompt charmonia at forward rapidity, as demonstrated in Fig. 16 and [48, 49], surpassing Run 2 in precision and promising stronger constraints on quarkonium production mechanisms at LHC energies.

While charmonium and bottomonium states (not discussed) provide established probes, top-quark measurements open a new window onto the earliest QGP stages. The $t\bar{t}$ signal reported by ATLAS [51] observed with a significance of 5σ in dilepton channels, is consistent with earlier CMS data [52] and nPDF predictions. This observation consolidates evidence for the presence of all quark flavors in the pre-equilibrium QGP stage at the LHC energies and paves the way for further time-resolved studies of the QGP formation and dynamics.

8 Ultra-peripheral collisions

The search for gluon saturation remains a central question in QCD. Although many observables have been proposed, existing measurements can often be explained without invoking saturation. Ultra-peripheral collisions (UPC) offer a sensitive probe, allowing studies of vector meson photoproduction over broad kinematics, revealing strong nuclear modifications of cross sections and testing gluon distribution models. At the conference, ALICE and CMS presented results on incoherent J/ψ photoproduction. Fig. 17 shows the ALICE measurement [53, 54], the first multi-differential study of incoherent J/ψ production as a function of

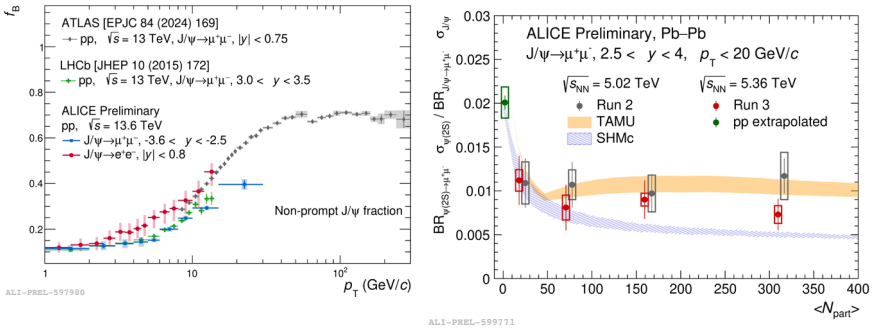

Figure 16. ALICE preliminary Run 3 results on J/ψ fraction originating from B-hadron decays in pp collisions [48] (left) and centrality dependence of $\psi(2S)$-to-J/ψ compared with Run 2 results, other experiments aand models [49]. Figures adopted from [48, 49].

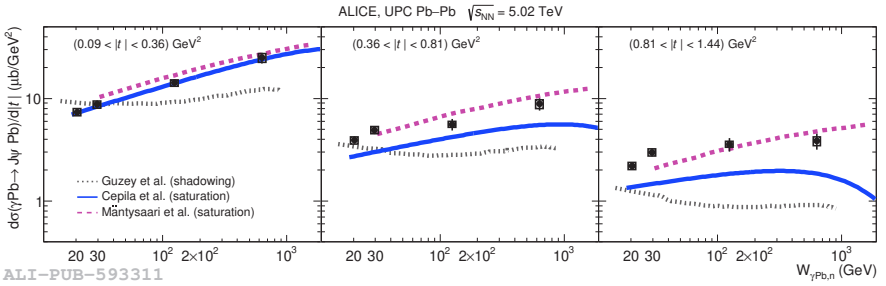

Figure 17. The energy dependence of the cross section of incoherent J/ψ photonuclear production off Pb nuclei as a function of the Mandelstam-t compared with models. Figure adopted from [53, 54].

energy and momentum transfer $|t|$ in ultra-peripheral Pb+Pb collisions at $\sqrt{s_{NN}}$ = 5.02 TeV, extending CMS data [55]. The cross section increases with energy for all $|t|$, but the increase is strongly suppressed at large $|t|$, corresponding to small gluonic configurations. This $|t|$-dependent suppression, not explained by leading-twist nuclear shadowing, is qualitatively reproduced by saturation-based models, suggesting the onset of gluon saturation at subnucleonic scales. A growing UPC program is also exploring charm production to probe parton dynamics. CMS measured inclusive D^0 meson production for p_T = 2–5 GeV/c (Fig. 18) [56]. The observed rapidity-dependent suppression relative to proton PDFs indicates reduced low-x gluon densities, while predictions using EPPS21 and nNNPDF3.0 slightly overestimate but remain consistent with the data. Preliminary ALICE Run 3 results further extend the D^0 measurements to lower p_T, providing new constraints on CNM effects at low x and Q^2.

Finally, UPCs offer a unique environment to search for QGP-like behavior in small systems. In past, ATLAS observed significant v_2 and v_3 flow in γ+Pb events [58], with v_2 smaller than in p+Pb collisions at comparable multiplicity. These results, interpretable through hydrodynamic or glasma-based frameworks, suggest similar radial flow across systems. The possible formation of a small QGP droplet could also manifest as baryon/meson and strangeness enhancement. This scenario was explored by ATLAS in photonuclear Pb+Pb collisions [57], which reveal mass-ordered $\langle p_T \rangle$ and enhanced Λ/K^0_S ratios at intermediate p_T (Fig. 18, right), both reminiscent of collective behavior. These features are not reproduced by models without final-state interactions but are well described by hybrid hydrodynamic approaches, suggesting QGP-like dynamics may emerge even in photonuclear collisions.

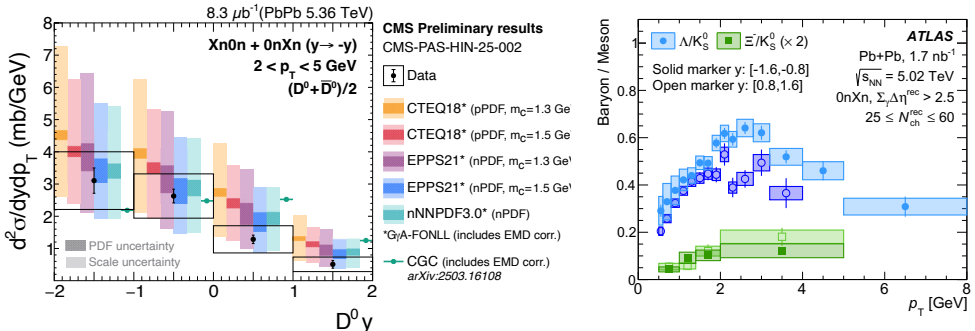

Figure 18. (Left) Rapidity dependence of D^0 cross-section in photonuclear Pb+Pb collisions at $\sqrt{s_{NN}}$ = 5.36 TeV measured by CMS [56]. (Right) Transverse momentum dependence of Λ/K^0_S yield ratio in photonuclear Pb+Pb collisions at $\sqrt{s_{NN}}$ = 5.02 TeV measured by ATLAS [57].

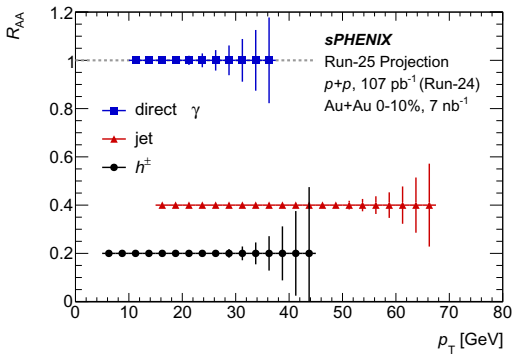

Figure 19. sPHENIX projections for R_{AA} measurements in Au+Au collisions at $\sqrt{s_{NN}}$ = 200 GeV based on data to be taken in Run25 at RHIC.

9 Outlook

Looking ahead, a number of exciting developments are expected in the coming years that will significantly advance the study of QCD matter. The final high-statistics data-taking campaign at RHIC will provide an unprecedented opportunity to explore QGP properties at energies complementary to those at the LHC with extended kinematic reach, marking the culmination of over two decades of discovery and bringing RHIC's mission to map the QCD phase diagram to its completion. In this context, sPHENIX is successfully taking data [59, 60] and will provide high-precision measurements of hard probes over an extended kinematic range, as demonstrated in the projected performance for the R_{AA} measurement (cf. Fig. 19). In parallel, STAR will continue to play a key role including its new forward physics program, offering important complementarity to future studies at the Electron–Ion Collider.

At the LHC, Run 3 is already delivering high-quality data with enhanced detector capabilities, and the upcoming Run 4 and HL-LHC phases will bring further improvements in statistical precision and detector performance. In parallel, several major detector upgrades are being planned or proposed to meet the demands of next-generation measurements. Among these, the ALICE 3 proposal [61] stands out as a dedicated heavy-ion experiment optimized for rare and low-p_T probes. It will open up new opportunities for measurements of low-p_T beaty-hadrons, multi-charm states, EM radiation down to ultrasoft photon energies, and E-by-E fluctuations such as net-baryon number, all key to probing the early QGP stages and its dynamics. In parallel, future facilities such as the CBM experiment at FAIR and proposed SPS-based programs (NA61/SHINE, NA60+/DiCE) at CERN will play a crucial role in exploring the high-baryon-density region of the QCD phase diagram, complementing the high-energy, low-μ_B studies at RHIC and the LHC.

These advances come at a moment of growing recognition for the field: the 2024 Breakthrough Prize in Fundamental Physics, awarded in part for the discovery of the QGP and the study of its properties, underscores the impact of heavy-ion physics on our understanding of the strong interaction and the early universe.

Acknowledgments

The work has been supported by the Czech Science Foundation grant 23-07499S. The author would also like to sincerely thank (in alphabetical order) F. Antinori, X. Bao, T. Boettcher, H. Caines, Yu-Chen (Janice) Chen, M. Connors, A. Dainese, G. Dale-Gau, D. Derendarz, H. Elfner, T. Galatyuk, F. Geurts, V. Humlová, G. M. Innocenti, J. Jia, A. Kudinoor, M. van Leeuwen, E. Lesser, Y.-J. Lie, G. Manca, D. Pablos, D. Perepelitsa, S. Radhakrishnan, K. Rajagopal, G. Roland, L. Ruan, M. Rybář, C. Soumik, M. Spousta, D. Tapia Takaki, B. Trzeciak, J. Velkovska, Zhiwan Xu, and H. Zbroszczyk for all insightful discussions, input, and help during the preparation of the presentation.

[1] H. Satz, R. Stock, Nucl. Phys. A **956**, 898 (2016). 10.1016/j.nuclphysa.2016.06.002
[2] B.E. Aboona et al. (STAR), Phys. Rev. Lett. **135**, 142301 (2025), 2504.00817. 10.1103/9l69-2d7p
[3] K. Grebieszkow et al. (NA61/SHINE), in *these proceedings*, 2508.15939
[4] H. Adhikary et al. (NA61/SHINE), Eur. Phys. J. C **85**, 918 (2025), 2503.22484. 10.1140/epjc/s10052-025-14621-z
[5] H. Zbroszczyk et al. (HADES), in *these proceedings*, 2510.19180
[6] M. Nabroth et al. (HADES), in *these proceedings*, 2510.15353
[7] T. Lu et al. (STAR), in *these proceedings*
[8] A. Hayrapetyan et al. (CMS), Phys. Rev. Lett. **135**, 132301 (2025), 2502.07898. 10.1103/6ywq-gm61
[9] B. Aboona et al. (STAR) (2025), 2506.05499.
[10] Z. Lu et al. (ALICE), in *these proceedings*
[11] G. Aad et al. (ATLAS), Phys. Rev. C **112**, 024910 (2025), 2412.15658. 10.1103/d46f-yl4n
[12] S. Acharya et al. (ALICE) (2024), 2411.09323.
[13] B.E. Aboona et al. (STAR), Phys. Rev. Lett. **135**, 072301 (2025), 2504.02531. 10.1103/2qhx-cp79
[14] S. Acharya et al. (ALICE) (2025), 2504.02359.
[15] R. Aaij et al. (LHCb) (2025), 2505.09273.
[16] Z. Yan et al. (STAR), in *these proceedings*, 2510.03454
[17] B. Schenke, C. Shen, D. Teaney, Phys. Rev. C **102**, 034905 (2020), 2004.00690. 10.1103/PhysRevC.102.034905
[18] G. Aad et al. (ATLAS) (2025), 2503.24125.
[19] S. Acharya et al. (ALICE) (2025), 2504.04796.
[20] K. Zhang et al. (STAR), in *these proceedings*
[21] X. Jiang et al. (STAR), in *these proceedings*
[22] L. Serksnyte et al. (ALICE), in *these proceedings*
[23] N.J. Abdulameer et al. (PHENIX), Phys. Rev. C **109**, 044912 (2024), 2203.17187. 10.1103/PhysRevC.109.044912
[24] N.J. Abdulameer et al. (PHENIX) (2025), 2504.02955.
[25] X. Bao et al. (STAR), in *these proceedings*
[26] S. Acharya et al. (ALICE), Phys. Lett. B **868**, 139645 (2025), 2411.14366. 10.1016/j.physletb.2025.139645
[27] J. Adamczewski-Musch et al. (HADES), Nature Phys. **15**, 1040 (2019). 10.1038/s41567-019-0583-8
[28] B.E. Aboona et al. (STAR), Nature Commun. **16**, 9098 (2025), 2402.01998. 10.1038/s41467-025-63216-5
[29] A. Andronic, P. Braun-Munzinger, K. Redlich, J. Stachel, Nature **561**, 321 (2018), 1710.09425. 10.1038/s41586-018-0491-6
[30] A. Bazavov et al. (HotQCD), Phys. Lett. B **795**, 15 (2019), 1812.08235. 10.1016/j.physletb.2019.05.013
[31] S. Borsanyi, Z. Fodor, J.N. Guenther, R. Kara, S.D. Katz, P. Parotto, A. Pasztor, C. Ratti, K.K. Szabo, Phys. Rev. Lett. **125**, 052001 (2020), 2002.02821. 10.1103/PhysRevLett.125.052001
[32] F. Eisenhut et al. (ALICE), in *these proceedings*

[33] T. Guo et al. (PHENIX), in *these proceedings*
[34] R. Aaij et al. (LHCb), Phys. Rev. D **112**, 072015 (2025), 2505.23530. 10.1103/r16d-b4my
[35] S. Acharya et al. (ALICE), Nature **605**, 440 (2022), [Erratum: Nature 607, E22 (2022)], 2106.05713. 10.1038/s41586-022-04572-w
[36] S. Zhang et al. (STAR), in *these proceedings*, 2510.18616
[37] A. Ray et al. (ALICE), in *these proceedings*
[38] V. Chekhovsky et al. (CMS), Phys. Lett. B **866**, 139556 (2025), 2503.19993. 10.1016/j.physletb.2025.139556
[39] A.S. Kudinoor, D. Pablos, K. Rajagopal (2025), 2509.08881.
[40] V. Chekhovsky et al. (CMS) (2025), 2507.09307.
[41] H. Bossi, A. Kudinoor, I. Moult, D. Pablos, A. Rai, K. Rajagopal, 2509.08047
[42] S.L. Cantway et al. (ALICE), in *these proceedings*
[43] G. Dale-Gau et al. (STAR), in *these proceedings*
[44] C. Wu et al. (ALICE), in *these proceedings*, 2509.02502
[45] CMS, https://cds.cern.ch/record/2932110
[46] V. Chekhovsky et al. (CMS), Phys. Rev. Lett. **135**, 092301 (2025), 2503.02139. 10.1103/c9wp-5tq3
[47] R. Aaij et al. (LHCb) (2025), 2506.08624.
[48] S. Acharya et al. (ALICE), in *these proceedings*
[49] S. Garetti et al. (ALICE), in *these proceedings*
[50] S. Acharya et al. (ALICE), Phys. Rev. Lett. **132**, 042301 (2024), 2210.08893. 10.1103/PhysRevLett.132.042301
[51] G. Aad et al. (ATLAS), Phys. Rev. Lett. **134**, 142301 (2025), 2411.10186. 10.1103/PhysRevLett.134.142301
[52] A.M. Sirunyan et al. (CMS), Phys. Rev. Lett. **125**, 222001 (2020), 2006.11110. 10.1103/PhysRevLett.125.222001
[53] S. Acharya et al. (ALICE) (2025), 2503.18708.
[54] V. Humlová et al. (ALICE), in *these proceedings*, 2510.11120
[55] V. Chekhovsky et al. (CMS), Phys. Rev. Lett. **135**, 112301 (2025), 2503.08903. 10.1103/w9kp-f8xr
[56] CMS, https://cds.cern.ch/record/2930669
[57] G. Aad et al. (ATLAS), Phys. Rev. C **111**, 064908 (2025), 2503.08181. 10.1103/7lx4-x8rw
[58] G. Aad et al. (ATLAS), Phys. Rev. C **104**, 014903 (2021), 2101.10771. 10.1103/PhysRevC.104.014903
[59] M.I. Abdulhamid et al. (sPHENIX), JHEP **08**, 075 (2025), 2504.02240. 10.1007/JHEP08(2025)075
[60] M.I. Abdulhamid et al. (sPHENIX), Phys. Rev. C **112**, 024908 (2025), 2504.02242. 10.1103/h8d5-swg6
[61] ALICE, 2211.02491, https://cds.cern.ch/record/2803563